Article

Cell Reports

Suppression of Resting Metabolism by the Angiotensin AT_2 Receptor

Graphical Abstract

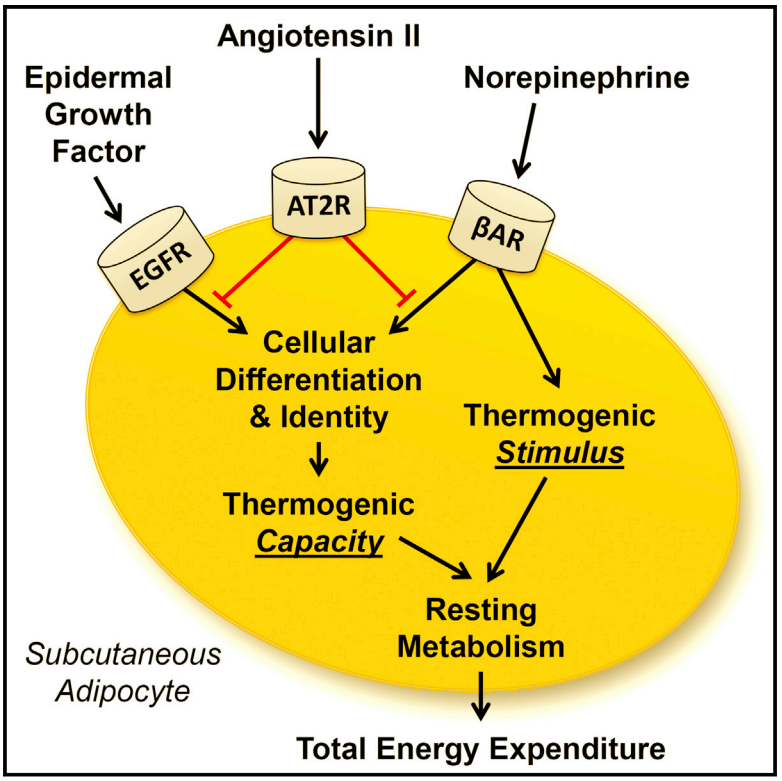

Authors

Nicole K. Littlejohn, Henry L. Keen, Benjamin J. Weidemann, ..., Kamal Rahmouni, Curt D. Sigmund, Justin L. Grobe

Correspondence

curt-sigmund@uiowa.edu (C.D.S.), justin-grobe@uiowa.edu (J.L.G.)

In Brief

The renin-angiotensin system has been implicated in tissue-specific actions underlying energy balance physiology. Littlejohn et al. document a major role for the angiotensin AT_2 receptor in the regulation of resting metabolism, through the control of differentiation and thermogenic capacity of subcutaneous adipocytes.

Highlights

- Angiotensin controls energy balance through opposing effects in brain and adipose tissue
- Angiotensin inhibits resting metabolism via its AT_2 receptor
- AT_2 activation interferes with UCP1 transcription, but not lipolysis, in adipocytes
- AT_2 interferes with altered adipocyte differentiation by epidermal growth factor

Accession Numbers

GSE77214

Littlejohn et al., 2016, Cell Reports *16*, 1548–1560
August 9, 2016
http://dx.doi.org/10.1016/j.celrep.2016.07.003

OPEN ACCESS
CellPress

Cell Reports
Article

Suppression of Resting Metabolism by the Angiotensin AT_2 Receptor

Nicole K. Littlejohn,[1] Henry L. Keen,[1] Benjamin J. Weidemann,[1] Kristin E. Claflin,[1] Kevin V. Tobin,[1] Kathleen R. Markan,[1] Sungmi Park,[1] Meghan C. Naber,[1] Francoise A. Gourronc,[2] Nicole A. Pearson,[1] Xuebo Liu,[1] Donald A. Morgan,[1] Aloysius J. Klingelhutz,[2,3] Matthew J. Potthoff,[1,3,4] Kamal Rahmouni,[1,3,4,5,6] Curt D. Sigmund,[1,3,4,5,6,*] and Justin L. Grobe[1,3,4,5,6,*]

[1]Department of Pharmacology
[2]Department of Microbiology
[3]Fraternal Order of Eagles' Diabetes Research Center
[4]Obesity Research and Education Initiative
[5]François M. Abboud Cardiovascular Research Center
[6]Center for Hypertension Research
University of Iowa, Iowa City, IA 52242, USA
*Correspondence: curt-sigmund@uiowa.edu (C.D.S.), justin-grobe@uiowa.edu (J.L.G.)
http://dx.doi.org/10.1016/j.celrep.2016.07.003

SUMMARY

Activation of the brain renin-angiotensin system (RAS) stimulates energy expenditure through increasing of the resting metabolic rate (RMR), and this effect requires simultaneous suppression of the circulating and/or adipose RAS. To identify the mechanism by which the peripheral RAS opposes RMR control by the brain RAS, we examined mice with transgenic activation of the brain RAS (sRA mice). sRA mice exhibit increased RMR through increased energy flux in the inguinal adipose tissue, and this effect is attenuated by angiotensin II type 2 receptor (AT_2) activation. AT_2 activation in inguinal adipocytes opposes norepinephrine-induced uncoupling protein-1 (UCP1) production and aspects of cellular respiration, but not lipolysis. AT_2 activation also opposes inguinal adipocyte function and differentiation responses to epidermal growth factor (EGF). These results highlight a major, multifaceted role for AT_2 within inguinal adipocytes in the control of RMR. The AT_2 receptor may therefore contribute to body fat distribution and adipose depot-specific effects upon cardio-metabolic health.

INTRODUCTION

The renin-angiotensin system (RAS) is well recognized for its varied roles in cardiovascular physiology. Increasing evidence also supports tissue-specific actions of angiotensin II (ANG) in the control of energy balance. Human obesity is associated with increased activity of the circulating RAS (Engeli et al., 2005), and various studies have documented beneficial effects of RAS inhibition upon glycemic control endpoints in obese humans (Grassi et al., 2003; Hsueh et al., 2010; Lindholm et al., 2003; Shimabukuro et al., 2007). In rodent models, pharmacological or genetic interference with the RAS also generally has beneficial effects upon body mass (as reviewed recently [Claflin and Grobe, 2015; Littlejohn and Grobe, 2015]). It is therefore confusing that RAS blockade does not have an overt effect upon body mass in humans. We hypothesize that the multifaceted contribution of the RAS to energy balance (through opposing effects on intake and activity behaviors, digestive efficiency, and resting metabolic rate [RMR]) may result in a net caloric balance in humans and thereby no change in body mass. Understanding the tissue-specific molecular mechanisms by which the RAS mediates control of individual components of energy balance, such as RMR, will allow for the development of novel therapeutics for obesity and its sequelae.

While RAS-mediated mechanisms controlling food intake, digestive efficiency, and physical activity have been defined, RMR control by the RAS is much more complicated with tissue- and receptor-specific actions of ANG functioning in apparent opposition (Claflin and Grobe, 2015; Grobe et al., 2013). Stimulation of the brain RAS by transgenic activation, intracerebroventricular (ICV) infusion of ANG, or deoxycorticosterone acetate (DOCA)-salt treatment increase RMR through brain AT_1-dependent mechanisms (de Kloet et al., 2011, 2013; Grobe et al., 2010, 2011; Porter et al., 2003; Porter and Potratz, 2004). Oddly, chronic infusion of ANG in the periphery can reverse these effects of a stimulated brain RAS (Grobe et al., 2010), highlighting the opposing effects of the brain and peripheral versions of the RAS in energy homeostasis (Grobe et al., 2013). Thus, there remains a critical lack of understanding of the mechanisms that mediate control of RMR by the RAS and, in particular, how the brain RAS and peripheral RAS interact in this control. We hypothesize that while ANG acts within the brain to stimulate RMR, actions of ANG in the periphery suppress this mechanism of energy expenditure. The objective of the current project was therefore to clarify the mechanisms by which the peripheral RAS opposes the RMR-stimulating effects of the brain RAS.

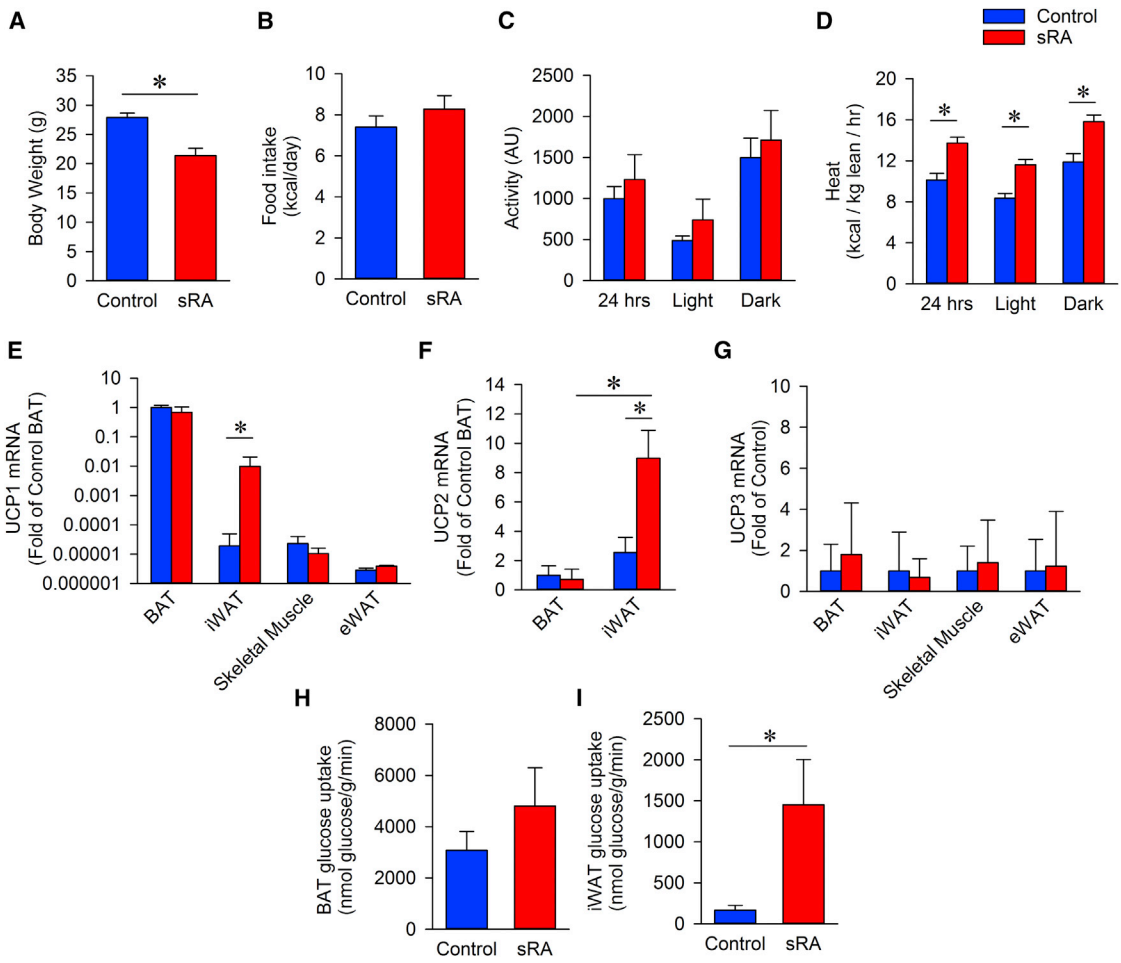

Figure 1. sRA Mice Exhibit Increased RMR Mediated by Inguinal White Adipose Tissue

(A–D) Body weight (A), food intake (B), activity (C), and heat production (D) as measured by respirometry in control and sRA mice (N = 8 per group; four males, four females).

(E) UCP1 mRNA in BAT, iWAT, skeletal muscle (gastrocnemius), and eWAT (N = 3).

(F) UCP2 mRNA in BAT and iWAT (N = 3).

(G) UCP3 mRNA in BAT, iWAT, skeletal muscle, and eWAT (N = 3).

(H) BAT glucose uptake in control (N = 8; four males, four females) and sRA (N = 7; three males, four females).

(I) iWAT glucose uptake in control (N = 8; four males, four females) and sRA (N = 7; three males, four females).

*$p < 0.05$ was considered significant. All data presented as mean ± SEM. See also Figure S1.

RESULTS

The Brain RAS Stimulates RMR

Double-transgenic "sRA" mice exhibit brain-specific elevations in RAS activity due to transgenic expression of both a human renin transgene via the synapsin promoter (sR) and a human angiotensinogen transgene under transcriptional control by its own promoter (A) (Sakai et al., 2007). Under baseline conditions, double-transgenic sRA mice exhibit decreased body weight and proportional fat mass compared to single- and non-transgenic littermate controls (Figure 1A; Table S1). Although these animals display normal food intake (Figure 1B) and physical activity (Figure 1C), sRA mice exhibit an elevated metabolic rate throughout the light-dark cycle (Figure 1D). These data confirm our previous studies of elevated energy expenditure in the sRA mouse model (Grobe et al., 2010, 2013) and those of our group and others studying pharmacological models of elevated brain RAS activity, including mice and rats with ICV infusion of ANG or DOCA-salt treatment (de Kloet et al., 2011; Grobe et al., 2011; Hilzendeger et al., 2013; Porter et al., 2003; Porter and Potratz, 2004). Collectively, these findings support a major stimulatory effect of the brain RAS upon RMR and thereby energy expenditure.

Selective Modulation of Inguinal Fat Function

We previously established that sRA mice exhibit increased thermogenesis as measured by core body temperature, adipose sympathetic nerve activity, and RMR when measured at thermoneutrality (Grobe et al., 2010). To identify the thermogenic tissue responsible for the increased RMR of sRA mice, we measured uncoupling protein-1 (UCP1) mRNA, which mediates

non-shivering thermogenesis in a variety of tissues (Shabalina et al., 2013). sRA mice demonstrated a significant (~500-fold) increase in UCP1 mRNA specifically within the inguinal white adipose tissue (iWAT); however, there was no change in UCP1 expression between sRA and control mice in interscapular brown adipose tissue (BAT), skeletal muscle, and epididymal fat (eWAT) (Figure 1E). We also examined the expression profile of UCP2, which has low expression in various tissues, and UCP3, which is more predominant in skeletal muscle and BAT (Vidal-Puig et al., 1997). The expression of UCP2 was not different between control and sRA mice in BAT, but was elevated in iWAT of sRA mice (Figure 1F). UCP3 expression was not changed between genotypes in BAT, iWAT, skeletal muscle, or eWAT (Figure 1G). These data point to the inguinal fat as the likely mediator of the elevated RMR in sRA mice.

Acknowledging that UCP1 mRNA or protein levels do not equate to energy flux or heat production (Nedergaard and Cannon, 2013), we next examined rates of glucose uptake in various tissues as a more direct assessment of energy flux. To analyze glucose uptake in tissues from control and sRA mice, we performed a glucose tracer test by injecting radiolabeled glucose ([^{3}H]2-deoxyglucose in 20% glucose solution). Glucose uptake in BAT (Figure 1H), heart (Figure S1A), and quadriceps skeletal muscle (Figure S1B) were not significantly different in sRA mice compared to control mice, though a trend toward a possible increase in BAT was noted. In contrast, and complementing the above UCP1 gene expression data, iWAT exhibited a tremendous, 9-fold, increase in glucose uptake in sRA mice compared to littermate controls (Figure 1I). Thus, the elevated UCP1 expression in the inguinal fat is associated with an increase in energy flux specifically in this fat depot.

AT_2 Activation Suppresses Metabolic Rate

Previously we determined that the suppressed activity of the circulating RAS in sRA mice is essential for the increased RMR in these animals. Specifically, we found that chronic peripheral infusion of a low, non-pressor dose of ANG via subcutaneous minipump normalized the elevated RMR in these mice without effect in littermate controls (Grobe et al., 2010). The tissue and receptor type mediating this action of the exogenous ANG, however, remained unclear. To examine whether this effect was directly mediated through actions upon adipocytes or indirectly mediated through actions upon other tissues, and to identify the specific receptors that mediate this effect, we next examined the effects of ANG action in cultured adipocytes.

Blockade of the AT_1 receptor with losartan in differentiated 3T3-L1 adipocytes failed to alter UCP1 mRNA (Figure 2A). In contrast, antagonism of AT_2 with PD-123,319 appeared to increase UCP1 expression and low-dose activation of AT_2 with CGP-42112a (“CGP,” at doses where CGP maintains AT_2-selectivity [Hines et al., 2001] significantly suppressed UCP1 expression (Figure 2A). We confirmed the reduction of UCP1 expression following AT_2 activation by CGP treatment (10 nM) in differentiated primary adipocytes isolated from iWAT of neonatal wild-type C57BL/6J mice (Figure 2B). Collectively, these data support a direct, suppressive effect of adipocyte AT_2 receptors upon UCP1 mRNA. Given our in vivo data demonstrating a suppressive role for circulating ANG upon RMR in sRA mice (Grobe et al., 2010), we therefore hypothesized that selective activation of AT_2 receptors in sRA mice should normalize RMR and weight gain in these animals.

Control and sRA mice were chronically infused with saline or low-dose CGP (50 ng/kg/min, 8 weeks, s.c. [subcutaneously]) to test whether AT_2 activation is sufficient to normalize metabolic function in sRA mice. CGP infusion significantly increased sRA body mass (Figure 2C) without altering feeding behavior (Figure 2D). Caloric absorption through the gastrointestinal tract, as determined by bomb calorimetry, was also not different between sRA and littermate mice or with CGP treatment (Figure 2E), which was consistent with unaltered pancreatic lipase and colipase expression (Figure S2A). We concluded that AT_2 activation did not alter energy intake/uptake, but rather inhibited energy expenditure.

While chronic AT_2 activation had no effect on energy intake, this manipulation significantly reduced RMR in sRA mice (Figure 2F), consistent with a suppression of energy expenditure. Despite no change in the iWAT mass with CGP treatment (Table S2), the elevated UCP1 expression in this fat pad was normalized with CGP treatment in sRA mice (Figure 2G). Conversely, despite a reduction in whole-body RMR, CGP increased UCP1 mRNA in BAT (Figure S2B), further supporting a dominant role for inguinal fat in the observed energy balance changes of sRA mice. In addition to UCP1, the expression of brown or beige adipose markers (Wu et al., 2012) *Cidea* (Figure 2H) and *Eva1* (Figure 2I) were normalized in iWAT from sRA mice treated with CGP supporting further the concept that AT_2 activation reversed a “browning” of the iWAT in sRA mice. Interestingly, despite an increase in PGC-1α mRNA in iWAT of sRA mice, CGP did not alter PGC-1α expression (Figure 2J). In addition, analysis of brown or beige fat markers identified altered *Slc27a1*, *Sp100*, *Ear2*, *Tmem26*, *Cd40*, *Hspb7*, *Acot2*, and *Oplah* in the iWAT of sRA mice relative to control littermate mice, whereas *Ear2*, *Tbx1*, *Acot2*, and *Pdk4* were significantly changed with CGP (Figures S2C and S2D; Table S3). CGP did not have any significant effect upon any markers in wild-type control mice (Figures 2G–2J). Finally, with the exception of dermatopontin expression, which was suppressed in sRA mice and stimulated with CGP treatment, white adipose markers were largely unchanged in sRA mice (Table S4). These data support the concept that chronic AT_2 activation reduces RMR, likely through modulation of the molecular identity and thereby thermogenic program of the inguinal fat pad (iWA). Notably these findings do not exclude the possibility that CGP treatment may also modulate physical-activity-based energy expenditure; however, other studies have demonstrated small and opposing effects of AT_2 receptor modulation upon locomotor activity, reducing the likelihood of a major contribution of this mechanism to the energy balance changes noted herein (Gross et al., 2000; Hein et al., 1995; Watanabe et al., 1999). To further understand the mechanism of the RMR effects, we next investigated possible metabolic targets of AT_2.

AT_2 Modulation of RMR Is Not Mediated through Suppression of Sympathetic Nerve Activity

Sympathetic nerve activity (SNA) is known to mediate adaptive thermogenesis and thereby contribute to resting metabolism.

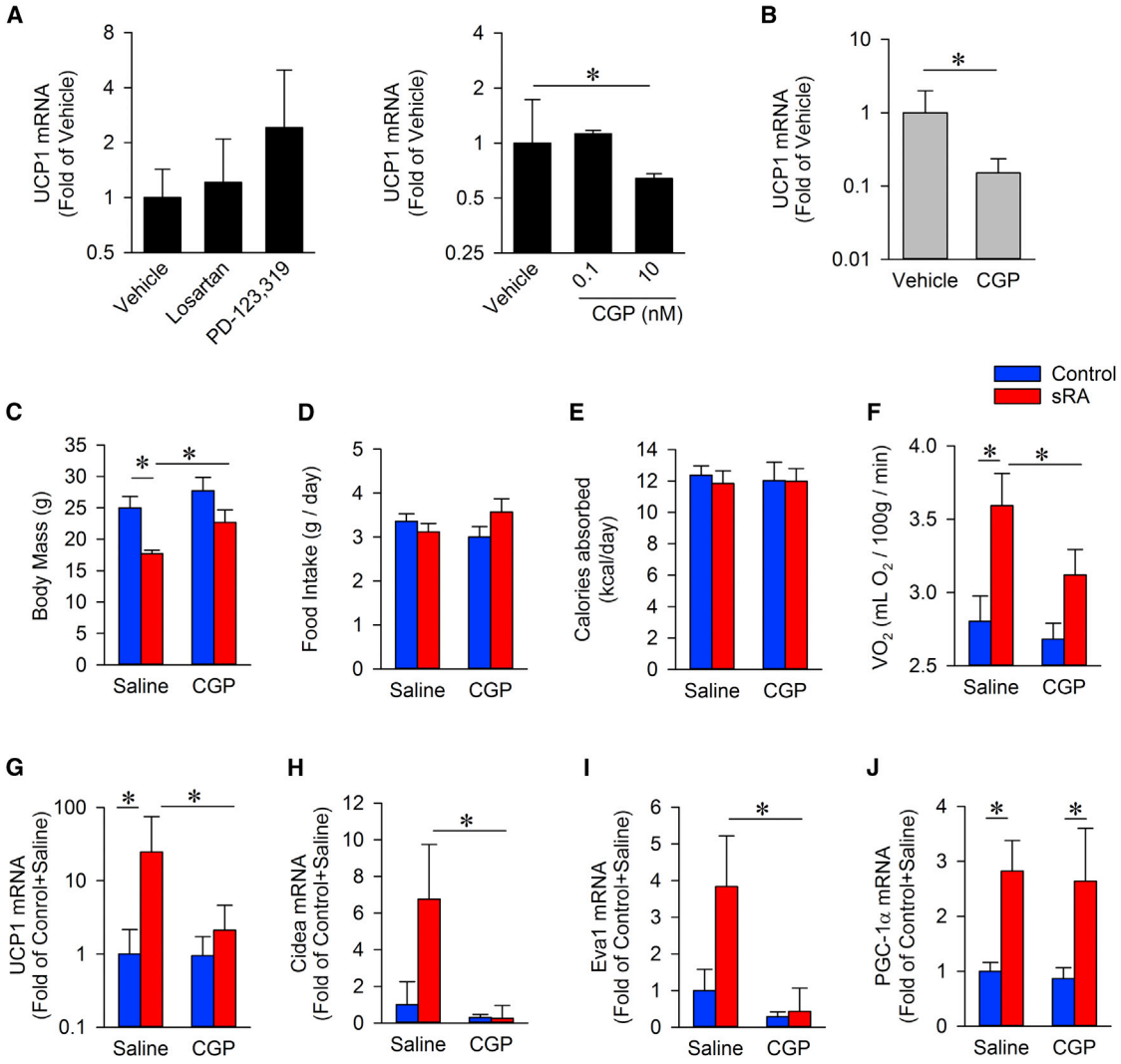

Figure 2. Chronic AT_2 Activation Reverses Metabolic Phenotypes of sRA Mice

(A) UCP1 mRNA from differentiated 3T3-L1 adipocytes treated with vehicle, losartan (10 μM), PD-123,319 (10 μM), or CGP-42112a "CGP" for 6 hr (N = 3 per treatment).

(B) UCP1 mRNA in mouse primary adipocytes isolated from iWAT in control mice treated with vehicle (N = 7) or CGP (10 nM; N = 7) for 6 hr.

(C–F) Body mass (C), daily food intake (D), calories absorbed via the gastrointestinal track (E), and oxygen consumption at thermoneutrality (F) in control and sRA mice treated with saline or CGP. Con+Sal, N = 5 (three males, two females); sRA+Sal, N = 5 (two males, three females); Con+CGP, N = 7 (four males, three females); sRA+CGP, N = 7 (four males, three females).

(G) UCP1 mRNA in the iWAT (N = 6).

(H) Cidea mRNA in the iWAT (N = 6).

(I) Eva1 mRNA in the iWAT (N = 6).

(J) PGC-1a mRNA in the iWAT (N = 6).

*$p < 0.05$ was considered significant. All data presented as mean ± SEM. See also Figures S2 and Tables S1 and S2.

Therefore, we hypothesized that AT_2 activation may reduce RMR through suppression of SNA. To test this, we recorded inguinal sympathetic nerve activity in littermate control or sRA mice following treatment with saline or the AT_2 agonist, CGP (Figure 3A). SNA to the iWAT was increased in sRA mice compared to littermate controls (Figures 3B and S3A). This is consistent with generalized increase in sympathetic activity as we previously documented, where renal and BAT SNA were elevated in sRA mice (Grobe et al., 2010). Somewhat unexpectedly, given its known suppressive functions within the central nervous system (Gao and Zucker, 2011), AT_2 activation via CGP infusion failed to reduce SNA in either genotype (Figures 3B and S3A). Additionally, we determined that while sRA mice exhibit various changes in blood pressure, heart rate, and renal renin expression, these endpoints were not significantly affected by CGP treatment in both control and sRA mice, possibly due to the low dose of CGP that was administered (Figures S3B and S3C).

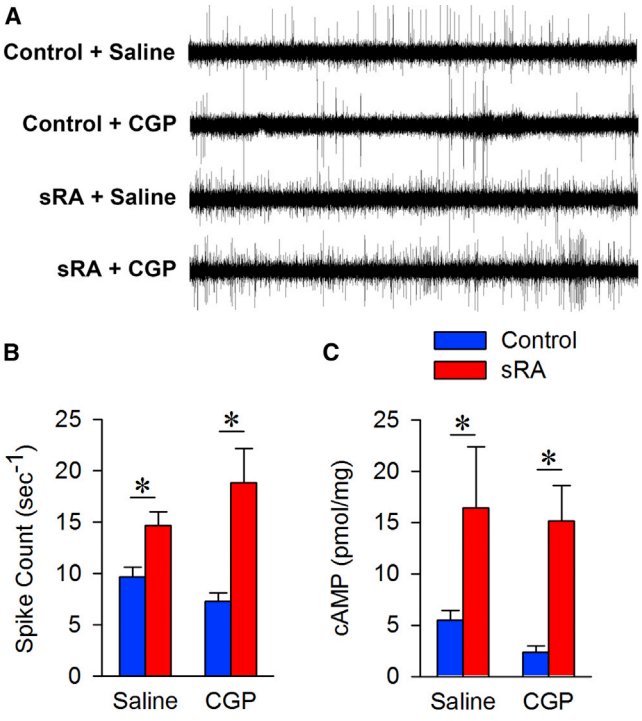

Figure 3. AT_2 Activation Does Not Reduce Inguinal SNA

(A) Representative electrograms from inguinal sympathetic nerves.

(B) Quantification of thresholded spike count. Con+Sal, N = 10 (three males, seven females); sRA+Sal, N = 10 (three males, seven females); Con+CGP, N = 8 each (two males, six females); sRA+CGP, N = 8 each (two males, six females).

(C) cAMP levels from iWAT isolated from control and sRA mice treated with saline or CGP (N = 3 per group).

*$p < 0.05$ was considered significant. All data presented as mean ± SEM. See also Figure S3.

Although the sympathetic drive to the iWAT was not suppressed with AT_2 activation, we next examined whether β-adrenergic signaling was altered within the iWAT. Therefore, we measured cAMP, which is produced upon β-adrenergic stimulation, within the iWAT. sRA mice exhibited elevated cAMP in the iWA, and cAMP levels remain high after AT_2 activation (Figure 3C). Hence, AT_2 activation does not reduce SNA or the immediate downstream signal of β-adrenergic stimulation within inguinal adipose. Rather, AT_2 likely may modulate other intracellular signal downstream of cAMP to suppress UCP1 transcription, glucose flux, and RMR within the iWAT.

AT_2 Receptor Activation Blunts Induction of UCP1 mRNA in White Adipocytes

To further investigate the mechanism of RMR modulation by AT_2 and to determine the effects of direct adipocyte-specific activation of AT_2, we examined second-messenger pathway functions in cultured primary adipocytes. Adipocytes from the iWA or the interscapular fat pad (BA) were isolated from neonatal wild-type C57BL/6J mice and cultured as reported previously (Markan et al., 2014). To examine the effect of activating AT_2 upon β-adrenergic signaling, we first assessed cAMP production in response to norepinephrine (NE; 10 μM) with or without CGP (10 nM) co-treatment. NE increased cAMP as expected in iWA, and CGP did not alter this effect (Figure 4A), which was consistent with our in vivo findings (Figure 3C). NE is also known to induce lipolysis, and liberated fatty acids are required to functionally activate UCP1 protein and to stimulate heat production (Atgié et al., 1997). Therefore, we considered the possibility that AT_2 may suppress lipolysis, ultimately suppressing heat production. Glycerol levels in the media of the cells were increased with NE treatment, but not altered with CGP in mouse iWA (Figure 4B) or BA (Figure S4A). We conclude that AT_2 does not modulate adipocyte cAMP production or lipolysis in response to NE.

Although lipolysis (and by extension UCP1 "activity") is not modulated by AT_2 activation, our data above support the modulation of UCP1 mRNA expression by AT_2 receptors. Activation of AT_2 did not alter NE-induced UCP1 mRNA in cultured mouse BA (Figure S4B). In contrast, the induction of UCP1 mRNA by NE was significantly blunted with CGP treatment in mouse iWA (Figure 4C). In a third adipose cell culture model consisting of immortalized human subcutaneous preadipocytes (Gadupudi et al., 2015; Vu et al., 2013, 2015), we confirmed a suppressive effect of AT_2 activation upon UCP1 mRNA (Figure 4D). These data support an action of AT_2 receptors to modulate β-adrenergic signaling downstream of cAMP production and the bifurcation of second-messenger modulation of UCP1 expression versus lipolysis. AT_2 is known to activate the serine/threonine phosphatase type 2A (PP2A) in other cell types (Shenoy et al., 1999), which led us to hypothesize that the modulatory effect of AT_2 activation in adipocytes may be mediated through phosphatase activity. Consistent with this possibility, we found that phosphatase inhibition with okadaic acid (OA) reversed the blunting effect of CGP on NE-induced UCP1 expression (Figure 4C). OA inhibits several phosphatases including PP1, PP2A, PP4, PP5, and PP6 (Swingle et al., 2007), and all of these were expressed at detectable levels in our RNaseq analysis of iWAs (Table S5). Similarly, the AT_2 antagonist, PD-123,319 (PD), also reversed the effects of AT_2 activation (Figure 4C). Together these data confirm the AT_2-dependent action of CGP in adipocytes to specifically modulate UCP1 expression (not activation) and implicate the activation of an OA-dependent phosphatase in this mechanism.

cAMP-response element binding protein (CREB) induces UCP1 transcription in response to elevated cAMP signaling (Rim and Kozak, 2002). Examination of known CREB target genes in the iWAT transcriptome via RNA sequencing (RNaseq) uncovered that 15 CREB targets had altered expression levels in control versus sRA mice and that the expression patterns of 7 of these genes were then significantly reversed with CGP treatment (Figure 4E; Table S6). CREB phosphorylation at Ser133 was increased after NE treatment and significantly attenuated with CGP co-treatment in mouse iWA (Figure 4F). Finally, antagonism of AT_2 activation by PD-123,319 disinhibited CREB binding to the UCP1 promoter in differentiated 3T3-L1 adipocytes in a chromatin immunoprecipitation assay (Figure 4G). Therefore, AT_2 likely blocks transcription of UCP1 through the phosphatase-mediated dephosphorylation and subsequent inactivation of the CREB transcription factor.

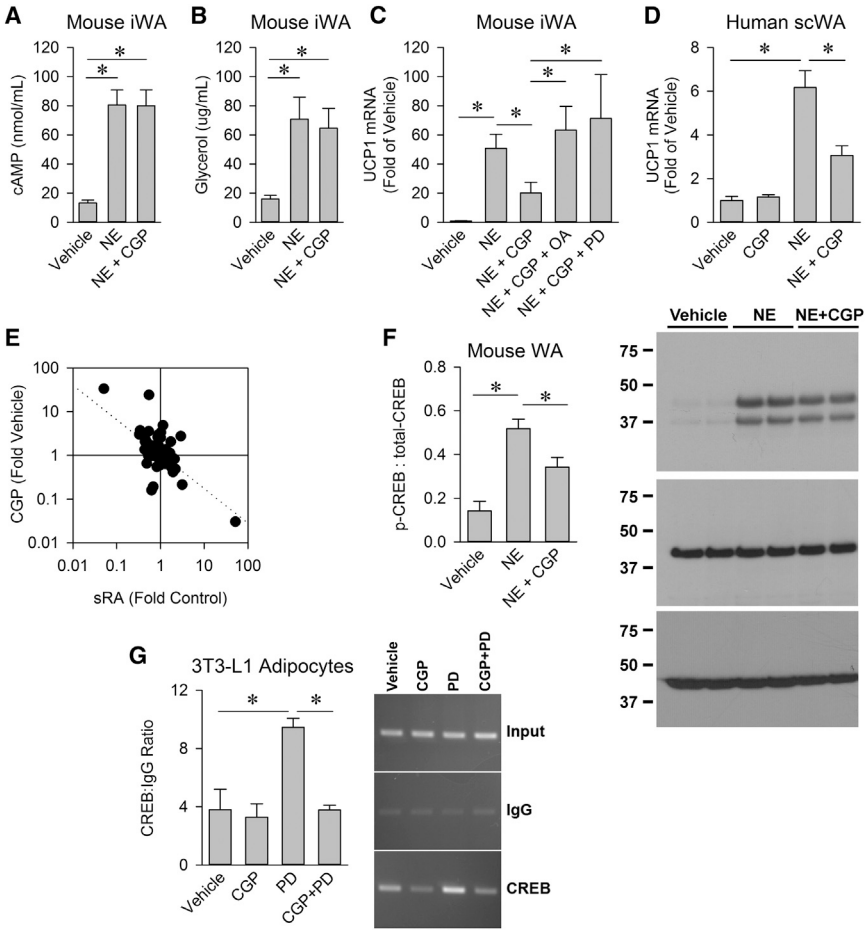

Figure 4. AT_2 Activation Suppresses Norepinephrine Induced UCP1 in White Adipocytes

(A) cAMP levels from mouse white adipocytes from iWAT (iWA) following treatment for 6 hr with vehicle, NE (10 μM), or NE and CGP (10 nM) (N = 6).

(B) Glycerol in the media from mouse iWA following treatment for 6 hr with vehicle, NE, or NE and CGP (N = 6).

(C) UCP1 mRNA in mouse iWA treatment for 6 hr (N = 7–8).

(D) UCP1 mRNA in human immortalized adipocytes following treatment for 6 hr with vehicle (N = 16), CGP (N = 11), NE (N = 9), or NE and CGP (N = 11).

(E) Expression of CREB target genes in iWAT transcriptome dataset.

(F) Representative western blot and quantification of western blot analysis of total and phosphorylated CREB in mouse iWA treated with vehicle, NE (1 μM), or NE + CGP (10 nM; N = 5 per group) for 5 min. β-actin served as a loading control.

(G) Chromatin immunoprecipitation assay for binding of CREB to the UCP1 promoter with CGP (10 nM) ± PD (10 μM); N = 3.

*$p < 0.05$ was considered significant. All data presented as mean ± SEM. See also Figure S4 and Table S3.

AT_2 Activation Does Not Decrease Canonical Natriuretic Peptide Signaling

Positive implication of an AT_2/phosphatase/CREB mechanism does not rule out other potential contributors to elevated RMR in sRA mice or other potential targets of AT_2 signaling in iWA. To probe these other potential mechanisms, we considered natriuretic peptide signaling, which has been reported to increase RMR and induce UCP1 in mice (Bordicchia et al., 2012). Upon atrial natriuretic peptide (ANP) or brain natriuretic peptide (BNP) binding to the signaling receptor, NPR-A, intracellular cGMP is produced. cGMP levels have been shown to be altered by AT_2 in other cell types (Bottari et al., 1992), raising the possibility that adipose natriuretic peptide signaling may be modulated by AT_2 signaling. Furthermore, chronic hypertension (as previously documented in sRA mice [Grobe et al., 2010; Littlejohn et al., 2013; Sakai et al., 2007]) has been correlated with increased levels of ANP (Sagnella et al., 1986) and BNP (Kohno et al., 1992). Thus, we assessed whether natriuretic peptide signaling is increased in sRA mice, and this may contribute to elevated RMR.

Total daily loss of ANP to urine (Figure 5A) was elevated in sRA mice even though no change in plasma ANP was detected (Figure S5A), supportive of an increased total daily ANP release. To determine if sensitivity to natriuretic peptide in iWAT was altered, we measured the expression of the canonical signaling receptor, NPR-A, and the clearance receptor, NPR-C. While NPR-A expression (Figure 5B) was not different, saline-treated sRA mice have decreased NPR-C mRNA (Figure 5C) compared to control mice. An enhanced signaling-to-clearance receptor mRNA ratio was proposed to indicate elevated sensitivity to natriuretic peptide signaling (Bordicchia et al., 2012). Therefore, the increased ratio of these receptor transcripts in iWAT of sRA mice (Figure 5D) may indicate greater sensitivity to natriuretic peptide signaling in sRA mice. CGP increased the expression of NPR-C and normalized the receptor ratio in sRA iWAT. As expected, iWAT cGMP levels were elevated in sRA mice, but surprisingly CGP did not reduce cGMP (Figure 5E). Thus, even though natriuretic peptide signaling appears to be enhanced in sRA iWAT and AT_2 activation increased the expression of the NPR-C clearance receptor, AT_2 activation does not suppress immediate second-messenger activation due to natriuretic peptide signaling. Therefore, the NPR-A/cGMP pathway is unlikely to mediate the observed effects of AT_2 activation upon UCP1 and RMR.

AT_2 Activation Reduces RMR via Suppression of Growth Factor Signaling

Next, we used an unbiased approach to identify additional signaling pathways that are altered in the iWAT of sRA mice. Specifically, we analyzed the transcriptome of iWAT from control and sRA mice treated with either saline or CGP, using RNA sequencing. From this examination, 123 genes were identified as having significantly altered expression ($p < 0.001$) between

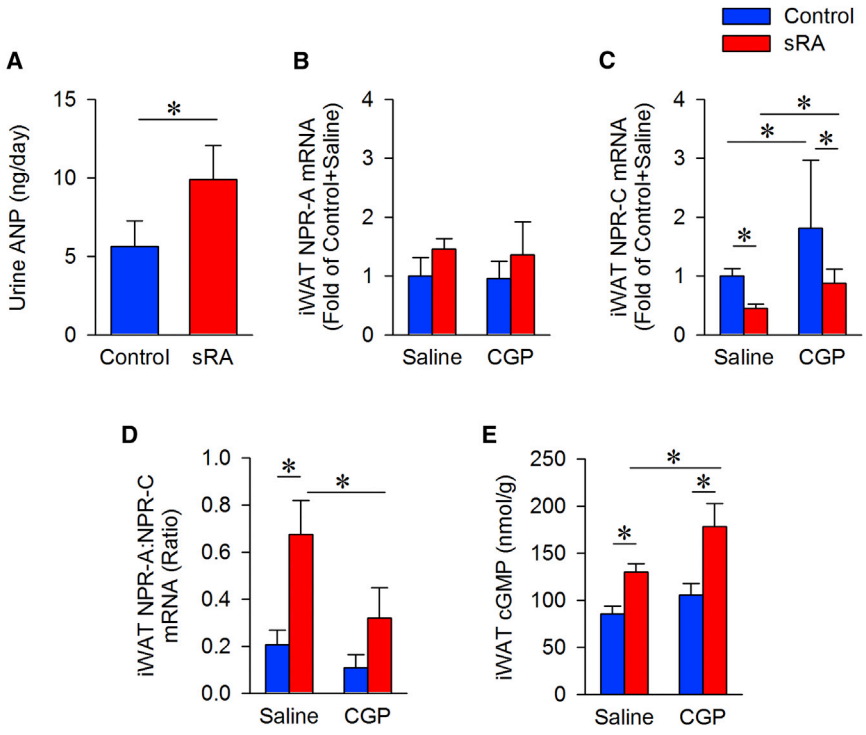

Figure 5. AT_2 Activation Does Not Suppress Canonical Natriuretic Peptide Signaling

(A) Urine ANP levels (N = 6; three males, three females).

(B) NPR-A mRNA in iWAT N = 4 per group (two males, two females).

(C) NPR-C mRNA in iWAT N = 4 per group (two males, two females).

(D) NPR-A to NPR-C mRNA ratio in iWAT N = 4 per group (two males, two females).

(E) cGMP levels in iWAT (N = 4; two males, two females).

*$p < 0.05$ was considered significant. All data presented as mean ± SEM. See also Figure S5.

control and sRA mice. Intriguingly, the alterations in expression of these same 123 genes were largely reversed with CGP treatment (Figure 6A). Gene set enrichment analysis (GSEA) (Subramanian et al., 2005) of the dataset uncovered that genes in the epidermal growth factor (EGF) signaling pathway were, as a group, upregulated (p value = 0.02) in sRA mice compared to littermate controls and suppressed (p value = 0.02) by CGP treatment. These data precipitated the hypothesis that AT_2 may additionally modulate RMR in sRA mice via interference with EGF signaling within the iWA.

To test if AT_2 targets EGF signaling to modulate RMR in vivo, we chronically infused wild-type C57BL/6J male mice for 2 weeks with saline, EGF (0.833 μg/hr, s.c.), CGP (50 ng/kg/min, s.c.), or both EGF and CGP. There was no significant change in body mass (Figure 6B), food intake (Figure 6C), or gastrointestinal caloric absorption (Figure 6D) in any treatment group during this relatively short-term treatment. In contrast, fat mass was reduced with EGF treatment, and this corresponded with an increase in lean body mass (Table S7). Critically, CGP co-treatment with EGF significantly reduced heat production compared to EGF alone (Figure 6E), though this co-treatment did not significantly alter the effect of 2-week EGF treatment upon adipose mass (Table S7). Therefore, AT_2 activation in wild-type mice is sufficient to reduce EGF-induced heat production.

To further examine the effects of AT_2 modulation upon RMR and the interaction between AT_2 and EGF in the control of RMR, we examined RMR control in mice genetically deficient for the AT_2 receptor (AT_2-KO), originally developed by Drs. Victor J. Dzau and Richard E. Pratt (Hein et al., 1995). Mice deficient for the AT_2 receptor, originally on the FVB/NCrl genetic background, were backcrossed onto the C57BL/6J background for > 7 generations before testing. RMR in a cohort of five male AT_2-KO (29.32 ± 1.62 g) and five weight-matched male littermate control mice (28.75 ± 1.52 g) was examined by respirometry. Although no change was observed in respiratory exchange ratio (RER; control 0.832 ± 0.010, AT_2-KO 0.833 ± 0.012), AT_2-KO mice exhibited a robust increase in RMR (control 0.217 ± 0.006 versus AT_2-KO 0.272 ± 0.019 kcal/hr, p = 0.02) (Figure S6).

We next tested the RMR responses of AT_2-KO mice and littermate controls to 2-week subcutaneous infusion of EGF. Body mass increased after EGF infusion in both littermate control (4.98 ± 0.36 g) and AT_2-KO (5.63 ± 0.35 g) mice compared to baseline, but this weight gain was reduced compared to untreated age-matched control and AT_2-KO mice (Figure 6F). Food intake (Figure 6G) and total caloric absorption (Figure 6H) were unchanged by treatment or genotype. EGF reduced iWAT and eWAT mass (Table S8), which is consistent with decreased adipose mass in EGF-treated rats (Pedersen et al., 2000; Serrero and Mills, 1991). Because of the wide differences in body weights between groups, we normalized heat production using analysis of covariance (ANCOVA) adjustment. As above, untreated AT_2-KO mice exhibited increased heat production compared to littermate controls under baseline conditions, consistent with a tonic inhibitory role for AT_2 in RMR control (Figure 6I). In addition, EGF increased heat production in both genotypes, but increased RMR in AT_2-KO mice to a much higher level than in littermate controls (Figure 6I). Therefore, we conclude that AT_2 receptors act as tonic suppressors of RMR, and this is related to alterations in EGF signaling.

Surprisingly, the mechanism of interaction between AT_2 and EGF in the adipose appears to be independent of modulation of UCP1 mRNA. UCP1 mRNA in the iWAT pad was unchanged (Figure S7A) or reduced (Figure S7B) by EGF infusion. In addition, we determined that UCP1 mRNA was unchanged by EGF treatment with or without co-treatment with the AT_2 antagonist, PD-123,319, in cultured adipocytes (Figure S7C), similar to our in vivo observations. In contrast, the effects of EGF upon adipocytes have largely been attributed to the modulation of differentiation (Hauner et al., 1995; Lee et al., 2008; Serrero, 1987). Thus,

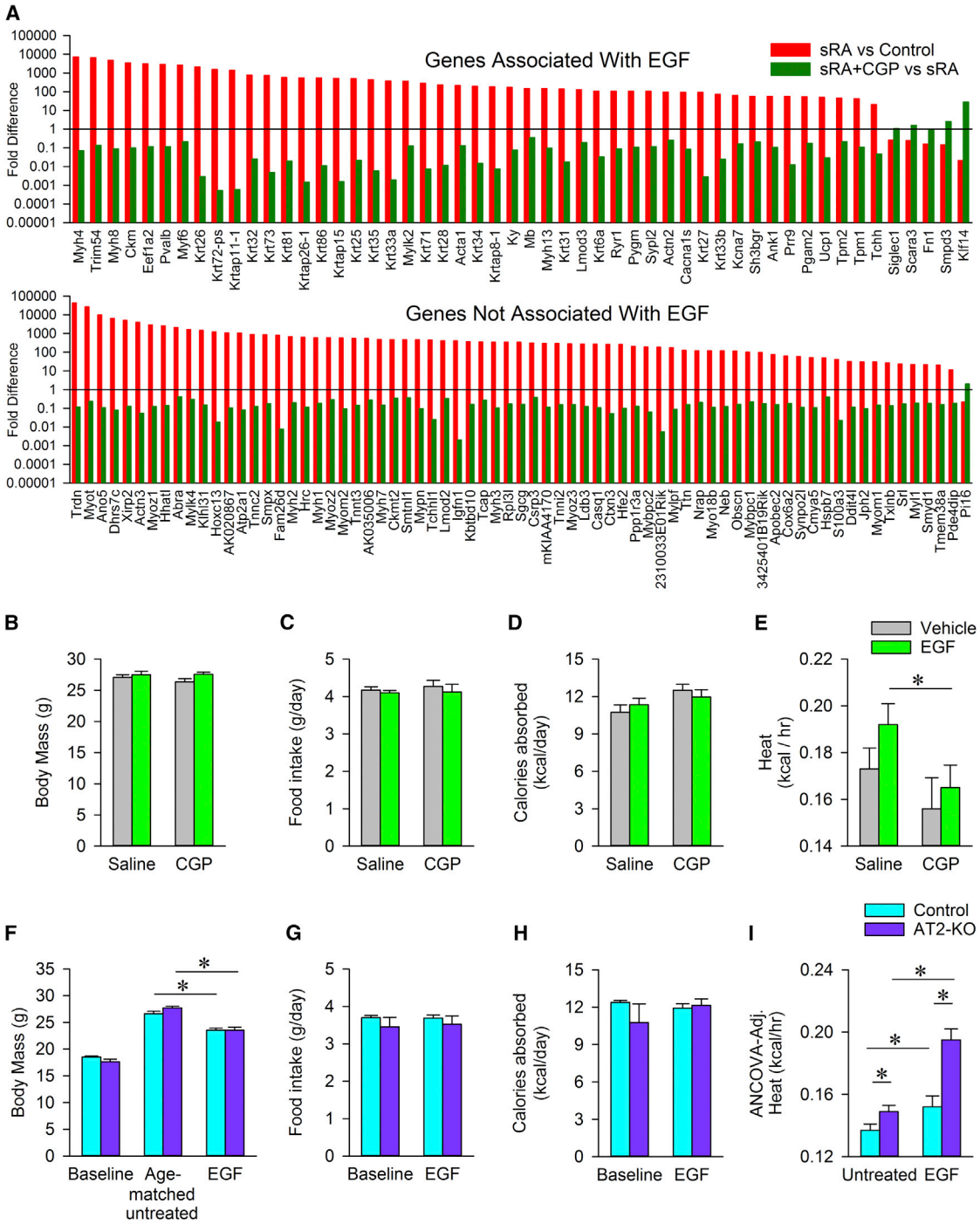

Figure 6. AT_2 Activation Suppresses EGF Signaling In Vivo

(A) Genes identified through RNA sequencing analysis from the iWAT isolated from control or sRA mice treated with saline or CGP. Top: includes genes known to be associated with EGF signaling. Bottom: genes not associated with EGF.

(B–E) Body mass (B), daily food intake (C), calories absorbed via the gastrointestinal tract (D), and heat as measured by respirometry (E) in wild-type C57BL/6J male mice treated for 2 weeks with saline (N = 20), EGF (N = 20), CGP (N = 9), or EGF and CGP (N = 17).

(F–I) Body mass (F), food intake (G), calories absorbed via the gastrointestinal track (H), or ANCOVA-adjusted heat production (I) in control and AT_2-KO mice (all males) at baseline, age-matched untreated control mice (N = 11), untreated AT_2-KO mice (N = 12), or after 2-week EGF treatment in control mice (N = 4) and AT_2-KO mice (N = 4).

*$p < 0.05$ was considered significant. All data presented as mean ± SEM. See also Figure S6 and Tables S4 and S5.

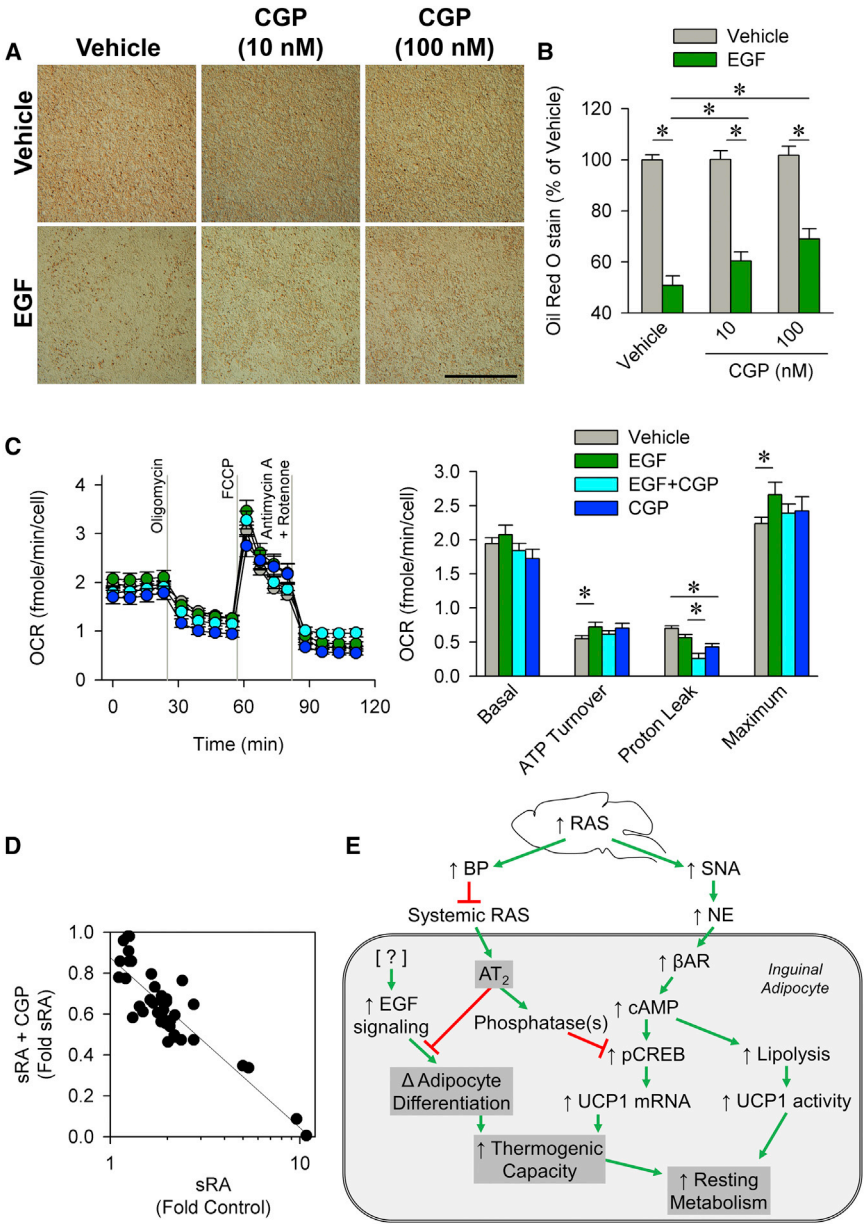

Figure 7. AT_2 Activation Reverses the Suppressed Adipogenesis by EGF

(A) Representative image of oil red O staining on day 4 of differentiation in mouse iWA treated with or without EGF (1 ng/mL) and/or CGP (10 or 100 nM). Scale bar, 1 mm.

(B) Quantification of oil red O staining (N = 5 per group).

(C) Oxygen consumption rate (OCR) in primary mouse WA treated with vehicle (N = 20), EGF (N = 10), or EGF and CGP (N = 20) during differentiation. Cells were subjected to a mitochondria stress test by acute stimulation with oligomycin, FCCP, and Antimycin A/Rotenone. WC, white adipocyte.

(D) Expression of electron transport genes identified as an enrichment set by GSEA in iWAT transcriptome-dataset.

(E) Model of elevated brain RAS and subsequent suppressed circulating RAS induction of resting metabolism.

*$p < 0.05$ was considered significant. All data presented as mean ± SEM. See also Table S6.

we examined the modulatory effect of CGP upon adipocyte differentiation. EGF treatment during differentiation resulted in a major suppression of adipocyte oil red O staining (Figure 7A). Consistent with the results above, CGP dose-dependently blunted the inhibitory effect of EGF on adipocyte differentiation (Figure 7B). To determine the functional significance of EGF-altered adipocyte differentiation, we measured oxygen consumption rate (OCR; normalized to cell number) in cells supplemented with EGF and/or CGP during differentiation (Figure 7C). Though EGF treatment had no significant effects upon basal OCR, CGP treatment significantly (main effect $p = 0.04$) suppressed basal OCR. Oligomycin treatment revealed a significant effect of CGP (main effect $p < 0.01$) to reduce proton leak consistent with a suppressive effect upon UCP1 expression in these cells. This major suppression of uncoupled proton leak by CGP (CGP alone was 62% of vehicle, and EGF+CGP was 46% of EGF alone) is consistent with the suppressive effect of CGP upon UCP1 and RMR in vivo (Figures 2F, 2G, 6E, and 6I). In addition, EGF increased ATP turnover by 32% in the absence of CGP (EGF × CGP interaction $p = 0.03$), consistent with a cross-talk between EGF and AT_2 in the control of electron transport chain activity. GSEA of the iWAT transcriptome from control and sRA mice treated with and without CGP (as presented in Figure 6A) uncovered a significant change in the expression of electron transport chain components (Figure 7D; Table S6). In the absence of CGP, EGF significantly increased maximal OCR responses to carbonyl cyanide-4-phenylhydrazone (FCCP) by 19% compared to vehicle, also supporting a major modulatory effect of EGF upon adipocyte thermogenic capacity. These data confirm physiologically significant and direct actions of both EGF and AT_2 within the inguinal adipocyte to modulate energy turnover and highlight complex interactions that may represent novel therapeutic targets for controlling adipocyte identity and function.

DISCUSSION

The implication of the RAS in the control of energy homeostasis in addition to its well-recognized role in cardiovascular functions may help clarify the comorbidity of metabolic and cardiovascular diseases, such as obesity and hypertension. The present study helps to illuminate the mechanisms involved in metabolic control

by the RAS. Specifically, we have documented actions of AT_2 receptor within inguinal adipocytes to control the molecular identity and thermogenic capacity of these cells (Figure 7E), ultimately to regulate whole-body energy balance. These insights help to clarify the nuanced and multifaceted effects of ANG in the periphery in the control of energy expenditure and the mechanisms of cross-talk between the brain and peripheral RAS. Future obesity therapeutics targeting the RAS may take advantage of the selective actions of ANG through the AT_2 receptor or its downstream targets specifically within subcutaneous adipose to modulate RMR and thereby energy homeostasis.

The adipose RAS contributes to obesity-hypertension, and adipose expansion is responsive to both the local adipose RAS and the circulating RAS (Goossens et al., 2003; Yvan-Charvet and Quignard-Boulangé, 2011). For example, transgenic overexpression of angiotensinogen specifically in adipose tissue causes mice to become hypertensive and obese (Yvan-Charvet et al., 2009). Yiannikouris et al. found that adipose-specific disruption of angiotensinogen prevents the induction of hypertension, but not weight gain, with diet-induced obesity (Yiannikouris et al., 2012a, 2012b). Consistent with these findings and the current study, Yvan-Charvet et al. previously demonstrated that genetic disruption of the AT_2 receptor prevented obesity but had no antihypertensive effect in mice overexpressing angiotensinogen in adipose tissue (Yvan-Charvet et al., 2005, 2009). Intriguingly, the actions of AT_2 to modulate UCP1 expression appear to be limited to the inguinal (subcutaneous) adipose pad. This discovery is interesting both mechanistically and for its clinical implications. As subcutaneous fat is largely considered "beneficial" opposed to inflammatory abdominal or visceral fat (Abate et al., 1995; McLaughlin et al., 2011; Miyazaki and DeFronzo, 2009), and as obesity is associated with increased circulating RAS activity (Engeli et al., 2005; Yasue et al., 2010), these findings implicate the adipose RAS in the modulation of cardio-metabolic risks during obesity.

The discovery of an interaction between AT_2 receptor signaling and EGF receptor signaling within adipocytes was not entirely unexpected. Others have previously documented a role for EGF in adipose development, and interactions between EGF and AT_2 have been reported in other tissues (Meffert et al., 1996; Nouet et al., 2004; Plouffe et al., 2006). Our data indicate that AT_2 stimulation impairs oxidative phosphorylation and highlight an important interaction between EGF and the AT_2 within inguinal adipocytes, but the molecular mechanism of this interaction remains elusive. Increased body mass index is correlated with a reduction in electron transport chain components resulting in decreased OCR in human adipocytes (Fischer et al., 2015). Thus, one possible mechanism for the elevated maximal oxidative phosphorylation observed with EGF treatment is an alteration in levels of electron transport chain components. Although further analysis of these mechanisms is warranted to determine how EGF and AT_2 modulate oxidative phosphorylation capacity, our data clearly support an interaction between EGF and the AT_2 receptor on adipocytes. Given our previous demonstration that the AT_2 receptor modulates anaerobic metabolism in vivo (Burnett and Grobe, 2013) and the previously established role for EGF in the modulation of anaerobic metabolism in cancer cells (Lee et al., 2015; Velpula et al., 2013), we posit that the molecular interaction between AT_2 and EGF within adipocytes may prove to be similar to that which occurs in cells exhibiting the Warburg effect. Another possible contributing mechanism may involve futile cycling of substrates such as creatinine, as this pathway has recently been documented as another UCP1-independent pathway of energy expenditure by adipocytes (Kazak et al., 2015).

Although no sex differences were noted in the current study, some data support a complex, sex-dependent contribution of AT_2 to the regulation of weight gain. Samuel et al. previously demonstrated that weight gain of AT_2-deficient mice on a high fat diet is normal in males but accelerated in females (Samuel et al., 2013). Nag et al. also previously demonstrated that pharmacological activation of the AT_2 receptor with C21 attenuated high-fat-diet-induced weight gain in female mice (Nag et al., 2015). How AT_2 may contribute to sex differences in susceptibility to weight gain, in terms of physiological mechanism (intake behavior, digestive efficiency, RMR, etc.) or molecular mechanism (activation of phosphatases, interference with EGFR signaling, etc.) remains unclear. Nonetheless, given the inguinal-fat-specific role for AT_2 action noted herein, a potential role for AT_2 in observed differences in adiposity and patterns of adipose distribution and adipose function (Blaak, 2001; Krotkiewski et al., 1983) between males and females could be speculated.

Ultimately these studies support the general concept that tissue- and receptor-specific actions of the RAS contribute to energy homeostasis (Littlejohn and Grobe, 2015). This overall concept likely helps to explain the lack of efficacy of "global" pharmacological RAS inhibition as a therapeutic approach to human obesity. Human obesity is correlated with increased circulating RAS activity (Engeli et al., 2005; Yasue et al., 2010), which would be expected to increase SNA (de Kloet et al., 2010). However, increased circulating RAS activity would presumably stimulate AT_2 signaling in thermogenic (or potentially thermogenic) adipose, resulting in reduced thermogenic capacity and thermogenesis in response to SNA stimulation. While pharmacological inhibition of the peripheral RAS could result in reduced adipose AT_2 activation, the loss of compartmentalization during obesity due to increased permeability of the blood-brain barrier (Gustafson et al., 2007) would simultaneously result in reduced brain RAS activation. The net effect on body mass would therefore be expected to be negligible. Future work to develop selective AT_2 antagonists that are incapable of crossing even a highly permeable blood-brain barrier may therefore prove useful for obesity therapeutics.

EXPERIMENTAL PROCEDURES

Experimental procedures are outlined in detail in the associated Supplemental Information.

Animals

All procedures performed were approved by the University of Iowa's Institutional Animal Care and Use Committee and conform to the guidelines set forth by the National Research Council (National Research Council, 2011). The sRA (sRA^{flox} line 11110/2 X 4284/1) transgenic colony was generated as previously described (Grobe et al., 2010; Sakai et al., 2007). Mice were treated with subcutaneous infusion of saline, CGP-42112a (100 ng/kg/min, s.c.), or EGF (AbD

Serotec; 0.833 μg/hr, s.c.) using Alzet osmotic minipumps. AT_2-KO mice, originally developed by Victor J. Dzau and Richard E. Pratt (Hein et al., 1995) were obtained from Charles River Laboratories on the FVB/NCrl background and were backcrossed onto the C57BL/6J background for at least seven generations. All animals had ad libitum access to standard chow (Harlan Teklad 7013) and water and were maintained on a standard 12:12 hr lighting cycle.

In Vivo Glucose Uptake Assay

Tail blood was collected from all mice (time = 0) followed by an injection (intraperitoneally [i.p.]) of 8–10 μCi of [3H]-2-deoxyglucose in a 20% glucose solution. Plasma radioactivity and [3H]-2-deoxyglucose uptake in tissues was analyzed as previously described (Markan et al., 2014).

Sympathetic Nerve Activity

Sympathetic nerve activity to the iWA was assessed as previously described (Grobe et al., 2010; Rahmouni et al., 2008).

Primary Adipocyte Culture

iWAT or interscapular BAT was collected from 4-day-old pups as previously described (Markan et al., 2014).

Immortalized Human Preadipocyte/Adipocyte Culture

Immortalized normal human preadipocytes (NPADs) have been described previously (Vu et al., 2013).

Cellular Respiration

Mouse primary inguinal white adipocytes were seeded and grown in XF96 V3 PET cell culture microplates (Seahorse Biosciences). OCR values were normalized to cell numbers as previously described (Wagner et al., 2011). The final mitochondrial inhibitor concentrations used were 2.5 μM oligomycin, 0.75 μM FCCP, 10 μM rotenone, and 10 μM Antimycin A.

RNA Sequencing Analysis

Total RNA was isolated from the iWA and was used to generate cDNA libraries with each library tagged with a unique sequence barcode. The libraries were sequenced (50-bp paired end reads) with the Illumina HiSeq 2000 at the DNA Facility at Iowa State University. The quality of the sequence reads was verified using the FastQC program. Bowtie (Langmead et al., 2009) was used to align sequences to the mouse genome (mm9, NCBI37) with alignment results saved in binary alignment map/sequence alignment map (BAM/SAM) format. The SortSam function of Picard Tools was used to sort SAM files and paired reads not mapping to the same genomic location were removed. The number of sequence reads per gene was calculated using the count function of gfold (Feng et al., 2012). The total counts per gene was normalized using the edgeR (Robinson et al., 2010) package in R/Bioconductor to account for the variance in the number of total sequence reads between samples. Statistical analysis of differential expression was done using the edgeR (Robinson et al., 2010), package and p value correction for multiple testing was done using the qvalue (Storey and Tibshirani, 2003) package in R/Bioconductor. An adjusted p value less than 0.001 was considered statistically significant.

Statistical Analyses

ANOVA (with or without repeated measures as appropriate) followed by Tukey multiple comparisons procedures were used throughout, with $p < 0.05$ considered statistically significant. ANCOVA was used to correct data for body mass, as indicated. Gene expression data were analyzed using the Livak method (Livak and Schmittgen, 2001). Mann-Whitney U, Kruskal-Wallis, or Friedman's ANOVA were used when data failed normality or equal variance tests, and their applications are noted in figure legends if used. Data are presented as mean ± SEM throughout.

ACCESSION NUMBERS

The accession number for the RNA sequencing data reported in this paper is GEO: GSE77214.

SUPPLEMENTAL INFORMATION

Supplemental Information includes Supplemental Experimental Procedures, seven figures, and nine tables and can be found with this article online at http://dx.doi.org/10.1016/j.celrep.2016.07.003.

AUTHOR CONTRIBUTIONS

N.K.L., H.L.K., B.J.W., K.E.C., K.V.T., K.R.M., M.C.N, F.A.G., N.A.P., X.L., D.A.M., and A.J.K. performed research and analyzed data. N.K.L. and J.L.G. drafted the manuscript. N.K.L., A.J.K., M.J.P., K.R., C.D.S., and J.L.G. revised the manuscript. All authors approved the final manuscript.

ACKNOWLEDGMENTS

The authors gratefully acknowledge technical assistance by the University of Iowa Genome Editing Core Facility, the Office of Animal Resources of the University of Iowa, Brett Wagner for technical assistance, and the intellectual support of Allyn L. Mark, MD. N.K.L. was supported by a predoctoral fellowship from the American Heart Association (14PRE18330015). B.J.W. was supported by undergraduate fellowships from the American Heart Association, the American Physiological Society, and the University of Iowa Center for Research by Undergraduates (ICRU). K.E.C. was supported by a predoctoral fellowship from the American Heart Association (14PRE20380401). K.R.M. was supported by a postdoctoral fellowship from the NIH (F32DK102347). This work was supported by grants from the NIH (DK106104 to M.J.P.; HL084207 to K.R., C.D.S., and J.L.G.; HL048058 to C.D.S.; HL098276 to J.L.G.), the American Diabetes Association (7-13-JF-49 to M.J.P.; 1-14-BS-079 to J.L.G.), the American Heart Association (14EIA18860041 to K.R.; 14IRG18710013 and 15SFRN23480000 to C.D.S.; and 15SFRN23730000 to J.L.G.), the University of Iowa's Vice President for Research and Economic Development (to J.L.G.), Roy J. Carver Trust (to C.D.S.), and Fraternal Order of Eagles' Diabetes Research Center (to A.J.K., M.J.P., and J.L.G.).

Received: February 8, 2016
Revised: June 9, 2016
Accepted: July 1, 2016
Published: July 28, 2016

REFERENCES

Abate, N., Garg, A., Peshock, R.M., Stray-Gundersen, J., and Grundy, S.M. (1995). Relationships of generalized and regional adiposity to insulin sensitivity in men. J. Clin. Invest. *96*, 88–98.

Atgié, C., D'Allaire, F., and Bukowiecki, L.J. (1997). Role of beta1- and beta3-adrenoceptors in the regulation of lipolysis and thermogenesis in rat brown adipocytes. Am. J. Physiol. *273*, C1136–C1142.

Blaak, E. (2001). Gender differences in fat metabolism. Curr. Opin. Clin. Nutr. Metab. Care *4*, 499–502.

Bordicchia, M., Liu, D., Amri, E.-Z., Ailhaud, G., Dessì-Fulgheri, P., Zhang, C., Takahashi, N., Sarzani, R., and Collins, S. (2012). Cardiac natriuretic peptides act via p38 MAPK to induce the brown fat thermogenic program in mouse and human adipocytes. J. Clin. Invest. *122*, 1022–1036.

Bottari, S.P., King, I.N., Reichlin, S., Dahlstroem, I., Lydon, N., and de Gasparo, M. (1992). The angiotensin AT2 receptor stimulates protein tyrosine phosphatase activity and mediates inhibition of particulate guanylate cyclase. Biochem. Biophys. Res. Commun. *183*, 206–211.

Burnett, C.M., and Grobe, J.L. (2013). Direct calorimetry identifies deficiencies in respirometry for the determination of resting metabolic rate in C57Bl/6 and FVB mice. Am. J. Physiol. Endocrinol. Metab. *305*, E916–E924.

Claflin, K.E., and Grobe, J.L. (2015). Control of energy balance by the brain renin-angiotensin system. Curr. Hypertens. Rep. *17*, 38.

de Kloet, A.D., Krause, E.G., and Woods, S.C. (2010). The renin angiotensin system and the metabolic syndrome. Physiol. Behav. *100*, 525–534.

de Kloet, A.D., Krause, E.G., Scott, K.A., Foster, M.T., Herman, J.P., Sakai, R.R., Seeley, R.J., and Woods, S.C. (2011). Central angiotensin II has catabolic action at white and brown adipose tissue. Am. J. Physiol. Endocrinol. Metab. *301*, E1081–E1091.

de Kloet, A.D., Pati, D., Wang, L., Hiller, H., Sumners, C., Frazier, C.J., Seeley, R.J., Herman, J.P., Woods, S.C., and Krause, E.G. (2013). Angiotensin type 1a receptors in the paraventricular nucleus of the hypothalamus protect against diet-induced obesity. J. Neurosci. *33*, 4825–4833.

Engeli, S., Böhnke, J., Gorzelniak, K., Janke, J., Schling, P., Bader, M., Luft, F.C., and Sharma, A.M. (2005). Weight loss and the renin-angiotensin-aldosterone system. Hypertension *45*, 356–362.

Feng, J., Meyer, C.A., Wang, Q., Liu, J.S., Shirley Liu, X., and Zhang, Y. (2012). GFOLD: a generalized fold change for ranking differentially expressed genes from RNA-seq data. Bioinformatics *28*, 2782–2788.

Fischer, B., Schöttl, T., Schempp, C., Fromme, T., Hauner, H., Klingenspor, M., and Skurk, T. (2015). Inverse relationship between body mass index and mitochondrial oxidative phosphorylation capacity in human subcutaneous adipocytes. Am. J. Physiol. Endocrinol. Metab. *309*, E380–E387.

Gadupudi, G., Gourronc, F.A., Ludewig, G., Robertson, L.W., and Klingelhutz, A.J. (2015). PCB126 inhibits adipogenesis of human preadipocytes. Toxicol. In Vitro *29*, 132–141.

Gao, L., and Zucker, I.H. (2011). AT2 receptor signaling and sympathetic regulation. Curr. Opin. Pharmacol. *11*, 124–130.

Goossens, G.H., Blaak, E.E., and van Baak, M.A. (2003). Possible involvement of the adipose tissue renin-angiotensin system in the pathophysiology of obesity and obesity-related disorders. Obes. Rev. *4*, 43–55.

Grassi, G., Seravalle, G., Dell'Oro, R., Trevano, F.Q., Bombelli, M., Scopelliti, F., Facchini, A., Mancia, G., and Study, C.; CROSS Study (2003). Comparative effects of candesartan and hydrochlorothiazide on blood pressure, insulin sensitivity, and sympathetic drive in obese hypertensive individuals: results of the CROSS study. J. Hypertens. *21*, 1761–1769.

Grobe, J.L., Grobe, C.L., Beltz, T.G., Westphal, S.G., Morgan, D.A., Xu, D., de Lange, W.J., Li, H., Sakai, K., Thedens, D.R., et al. (2010). The brain Renin-angiotensin system controls divergent efferent mechanisms to regulate fluid and energy balance. Cell Metab. *12*, 431–442.

Grobe, J.L., Buehrer, B.A., Hilzendeger, A.M., Liu, X., Davis, D.R., Xu, D., and Sigmund, C.D. (2011). Angiotensinergic signaling in the brain mediates metabolic effects of deoxycorticosterone (DOCA)-salt in C57 mice. Hypertension *57*, 600–607.

Grobe, J.L., Rahmouni, K., Liu, X., and Sigmund, C.D. (2013). Metabolic rate regulation by the renin-angiotensin system: brain vs. body. Pflugers Arch. *465*, 167–175.

Gross, V., Milia, A.F., Plehm, R., Inagami, T., and Luft, F.C. (2000). Long-term blood pressure telemetry in AT2 receptor-disrupted mice. J. Hypertens. *18*, 955–961.

Gustafson, D.R., Karlsson, C., Skoog, I., Rosengren, L., Lissner, L., and Blennow, K. (2007). Mid-life adiposity factors relate to blood-brain barrier integrity in late life. J. Intern. Med. *262*, 643–650.

Hauner, H., Röhrig, K., and Petruschke, T. (1995). Effects of epidermal growth factor (EGF), platelet-derived growth factor (PDGF) and fibroblast growth factor (FGF) on human adipocyte development and function. Eur. J. Clin. Invest. *25*, 90–96.

Hein, L., Barsh, G.S., Pratt, R.E., Dzau, V.J., and Kobilka, B.K. (1995). Behavioural and cardiovascular effects of disrupting the angiotensin II type-2 receptor in mice. Nature *377*, 744–747.

Hilzendeger, A.M., Cassell, M.D., Davis, D.R., Stauss, H.M., Mark, A.L., Grobe, J.L., and Sigmund, C.D. (2013). Angiotensin type 1a receptors in the subfornical organ are required for deoxycorticosterone acetate-salt hypertension. Hypertension *61*, 716–722.

Hines, J., Heerding, J.N., Fluharty, S.J., and Yee, D.K. (2001). Identification of angiotensin II type 2 (AT2) receptor domains mediating high-affinity CGP 42112A binding and receptor activation. J. Pharmacol. Exp. Ther. *298*, 665–673.

Hsueh, W., Davidai, G., Henry, R., and Mudaliar, S. (2010). Telmisartan effects on insulin resistance in obese or overweight adults without diabetes or hypertension. J. Clin. Hypertens. (Greenwich) *12*, 746–752.

Kazak, L., Chouchani, E.T., Jedrychowski, M.P., Erickson, B.K., Shinoda, K., Cohen, P., Vetrivelan, R., Lu, G.Z., Laznik-Bogoslavski, D., Hasenfuss, S.C., et al. (2015). A creatine-driven substrate cycle enhances energy expenditure and thermogenesis in beige fat. Cell *163*, 643–655.

Kohno, M., Horio, T., Yokokawa, K., Murakawa, K., Yasunari, K., Akioka, K., Tahara, A., Toda, I., Takeuchi, K., Kurihara, N., et al. (1992). Brain natriuretic peptide as a cardiac hormone in essential hypertension. Am. J. Med. *92*, 29–34.

Krotkiewski, M., Björntorp, P., Sjöström, L., and Smith, U. (1983). Impact of obesity on metabolism in men and women. Importance of regional adipose tissue distribution. J. Clin. Invest. *72*, 1150–1162.

Langmead, B., Trapnell, C., Pop, M., and Salzberg, S.L. (2009). Ultrafast and memory-efficient alignment of short DNA sequences to the human genome. Genome Biol. *10*, R25.

Lee, J.S., Suh, J.M., Park, H.G., Bak, E.J., Yoo, Y.J., and Cha, J.H. (2008). Heparin-binding epidermal growth factor-like growth factor inhibits adipocyte differentiation at commitment and early induction stages. Differentiation *76*, 478–487.

Lee, K.M., Nam, K., Oh, S., Lim, J., Lee, T., and Shin, I. (2015). ECM1 promotes the Warburg effect through EGF-mediated activation of PKM2. Cell. Signal. *27*, 228–235.

Lindholm, L.H., Persson, M., Alaupovic, P., Carlberg, B., Svensson, A., and Samuelsson, O. (2003). Metabolic outcome during 1 year in newly detected hypertensives: results of the Antihypertensive Treatment and Lipid Profile in a North of Sweden Efficacy Evaluation (ALPINE study). J. Hypertens. *21*, 1563–1574.

Littlejohn, N.K., and Grobe, J.L. (2015). Opposing tissue-specific roles of angiotensin in the pathogenesis of obesity, and implications for obesity-related hypertension. Am. J. Physiol. Regul. Integr. Comp. Physiol. *309*, R1463–R1473.

Littlejohn, N.K., Siel, R.B., Jr., Ketsawatsomkron, P., Pelham, C.J., Pearson, N.A., Hilzendeger, A.M., Buehrer, B.A., Weidemann, B.J., Li, H., Davis, D.R., et al. (2013). Hypertension in mice with transgenic activation of the brain renin-angiotensin system is vasopressin dependent. Am. J. Physiol. Regul. Integr. Comp. Physiol. *304*, R818–R828.

Livak, K.J., and Schmittgen, T.D. (2001). Analysis of relative gene expression data using real-time quantitative PCR and the 2(-Delta Delta C(T)) Method. Methods *25*, 402–408.

Markan, K.R., Naber, M.C., Ameka, M.K., Anderegg, M.D., Mangelsdorf, D.J., Kliewer, S.A., Mohammadi, M., and Potthoff, M.J. (2014). Circulating FGF21 is liver derived and enhances glucose uptake during refeeding and overfeeding. Diabetes *63*, 4057–4063.

McLaughlin, T., Lamendola, C., Liu, A., and Abbasi, F. (2011). Preferential fat deposition in subcutaneous versus visceral depots is associated with insulin sensitivity. J. Clin. Endocrinol. Metab. *96*, E1756–E1760.

Meffert, S., Stoll, M., Steckelings, U.M., Bottari, S.P., and Unger, T. (1996). The angiotensin II AT2 receptor inhibits proliferation and promotes differentiation in PC12W cells. Mol. Cell. Endocrinol. *122*, 59–67.

Miyazaki, Y., and DeFronzo, R.A. (2009). Visceral fat dominant distribution in male type 2 diabetic patients is closely related to hepatic insulin resistance, irrespective of body type. Cardiovasc. Diabetol. *8*, 44.

Nag, S., Khan, M.A., Samuel, P., Ali, Q., and Hussain, T. (2015). Chronic angiotensin AT2R activation prevents high-fat diet-induced adiposity and obesity in female mice independent of estrogen. Metabolism *64*, 814–825.

National Research Council (2011). Guide for the Care and Use of Laboratory Animals (National Academies Press).

Nedergaard, J., and Cannon, B. (2013). UCP1 mRNA does not produce heat. Biochim. Biophys. Acta *1831*, 943–949.

Nouet, S., Amzallag, N., Li, J.M., Louis, S., Seitz, I., Cui, T.X., Alleaume, A.M., Di Benedetto, M., Boden, C., Masson, M., et al. (2004). Trans-inactivation of

receptor tyrosine kinases by novel angiotensin II AT2 receptor-interacting protein, ATIP. J. Biol. Chem. *279*, 28989–28997.

Pedersen, S.B., Kristensen, K., Bruun, J.M., Flyvbjerg, A., Vinter-Jensen, L., and Richelsen, B. (2000). Systemic administration of epidermal growth factor increases UCP3 mRNA levels in skeletal muscle and adipose tissue in rats. Biochem. Biophys. Res. Commun. *279*, 914–919.

Plouffe, B., Guimond, M.O., Beaudry, H., and Gallo-Payet, N. (2006). Role of tyrosine kinase receptors in angiotensin II AT2 receptor signaling: involvement in neurite outgrowth and in p42/p44mapk activation in NG108-15 cells. Endocrinology *147*, 4646–4654.

Porter, J.P., and Potratz, K.R. (2004). Effect of intracerebroventricular angiotensin II on body weight and food intake in adult rats. Am. J. Physiol. Regul. Integr. Comp. Physiol. *287*, R422–R428.

Porter, J.P., Anderson, J.M., Robison, R.J., and Phillips, A.C. (2003). Effect of central angiotensin II on body weight gain in young rats. Brain Res. *959*, 20–28.

Rahmouni, K., Fath, M.A., Seo, S., Thedens, D.R., Berry, C.J., Weiss, R., Nishimura, D.Y., and Sheffield, V.C. (2008). Leptin resistance contributes to obesity and hypertension in mouse models of Bardet-Biedl syndrome. J. Clin. Invest. *118*, 1458–1467.

Rim, J.S., and Kozak, L.P. (2002). Regulatory motifs for CREB-binding protein and Nfe2l2 transcription factors in the upstream enhancer of the mitochondrial uncoupling protein 1 gene. J. Biol. Chem. *277*, 34589–34600.

Robinson, M.D., McCarthy, D.J., and Smyth, G.K. (2010). edgeR: a Bioconductor package for differential expression analysis of digital gene expression data. Bioinformatics *26*, 139–140.

Sagnella, G.A., Markandu, N.D., Shore, A.C., and MacGregor, G.A. (1986). Raised circulating levels of atrial natriuretic peptides in essential hypertension. Lancet *1*, 179–181.

Sakai, K., Agassandian, K., Morimoto, S., Sinnayah, P., Cassell, M.D., Davisson, R.L., and Sigmund, C.D. (2007). Local production of angiotensin II in the subfornical organ causes elevated drinking. J. Clin. Invest. *117*, 1088–1095.

Samuel, P., Khan, M.A., Nag, S., Inagami, T., and Hussain, T. (2013). Angiotensin AT(2) receptor contributes towards gender bias in weight gain. PLoS ONE *8*, e48425.

Serrero, G. (1987). EGF inhibits the differentiation of adipocyte precursors in primary cultures. Biochem. Biophys. Res. Commun. *146*, 194–202.

Serrero, G., and Mills, D. (1991). Physiological role of epidermal growth factor on adipose tissue development *in vivo*. Proc. Natl. Acad. Sci. USA *88*, 3912–3916.

Shabalina, I.G., Petrovic, N., de Jong, J.M., Kalinovich, A.V., Cannon, B., and Nedergaard, J. (2013). UCP1 in brite/beige adipose tissue mitochondria is functionally thermogenic. Cell Rep. *5*, 1196–1203.

Shenoy, U.V., Richards, E.M., Huang, X.C., and Sumners, C. (1999). Angiotensin II type 2 receptor-mediated apoptosis of cultured neurons from newborn rat brain. Endocrinology *140*, 500–509.

Shimabukuro, M., Tanaka, H., and Shimabukuro, T. (2007). Effects of telmisartan on fat distribution in individuals with the metabolic syndrome. J. Hypertens. *25*, 841–848.

Storey, J.D., and Tibshirani, R. (2003). Statistical significance for genomewide studies. Proc. Natl. Acad. Sci. USA *100*, 9440–9445.

Subramanian, A., Tamayo, P., Mootha, V.K., Mukherjee, S., Ebert, B.L., Gillette, M.A., Paulovich, A., Pomeroy, S.L., Golub, T.R., Lander, E.S., et al. (2005). Gene set enrichment analysis: a knowledge-based approach for interpreting genome-wide expression profiles. Proc. Natl. Acad. Sci. USA *102*, 15545–15550.

Swingle, M., Ni, L., and Honkanen, R.E. (2007). Small-molecule inhibitors of ser/thr protein phosphatases: specificity, use and common forms of abuse. Methods Mol. Biol. *365*, 23–38.

Velpula, K.K., Bhasin, A., Asuthkar, S., and Tsung, A.J. (2013). Combined targeting of PDK1 and EGFR triggers regression of glioblastoma by reversing the Warburg effect. Cancer Res. *73*, 7277–7289.

Vidal-Puig, A., Solanes, G., Grujic, D., Flier, J.S., and Lowell, B.B. (1997). UCP3: an uncoupling protein homologue expressed preferentially and abundantly in skeletal muscle and brown adipose tissue. Biochem. Biophys. Res. Commun. *235*, 79–82.

Vu, B.G., Gourronc, F.A., Bernlohr, D.A., Schlievert, P.M., and Klingelhutz, A.J. (2013). Staphylococcal superantigens stimulate immortalized human adipocytes to produce chemokines. PLoS ONE *8*, e77988.

Vu, B.G., Stach, C.S., Kulhankova, K., Salgado-Pabón, W., Klingelhutz, A.J., and Schlievert, P.M. (2015). Chronic superantigen exposure induces systemic inflammation, elevated bloodstream endotoxin, and abnormal glucose tolerance in rabbits: possible role in diabetes. MBio *6*, e02554.

Wagner, B.A., Venkataraman, S., and Buettner, G.R. (2011). The rate of oxygen utilization by cells. Free Radic. Biol. Med. *51*, 700–712.

Watanabe, T., Hashimoto, M., Okuyama, S., Inagami, T., and Nakamura, S. (1999). Effects of targeted disruption of the mouse angiotensin II type 2 receptor gene on stress-induced hyperthermia. J. Physiol. *515*, 881–885.

Wu, J., Boström, P., Sparks, L.M., Ye, L., Choi, J.H., Giang, A.H., Khandekar, M., Virtanen, K.A., Nuutila, P., Schaart, G., et al. (2012). Beige adipocytes are a distinct type of thermogenic fat cell in mouse and human. Cell *150*, 366–376.

Yasue, S., Masuzaki, H., Okada, S., Ishii, T., Kozuka, C., Tanaka, T., Fujikura, J., Ebihara, K., Hosoda, K., Katsurada, A., et al. (2010). Adipose tissue-specific regulation of angiotensinogen in obese humans and mice: impact of nutritional status and adipocyte hypertrophy. Am. J. Hypertens. *23*, 425–431.

Yiannikouris, F., Gupte, M., Putnam, K., Thatcher, S., Charnigo, R., Rateri, D.L., Daugherty, A., and Cassis, L.A. (2012a). Adipocyte deficiency of angiotensinogen prevents obesity-induced hypertension in male mice. Hypertension *60*, 1524–1530.

Yiannikouris, F., Karounos, M., Charnigo, R., English, V.L., Rateri, D.L., Daugherty, A., and Cassis, L.A. (2012b). Adipocyte-specific deficiency of angiotensinogen decreases plasma angiotensinogen concentration and systolic blood pressure in mice. Am. J. Physiol. Regul. Integr. Comp. Physiol. *302*, R244–R251.

Yvan-Charvet, L., and Quignard-Boulangé, A. (2011). Role of adipose tissue renin-angiotensin system in metabolic and inflammatory diseases associated with obesity. Kidney Int. *79*, 162–168.

Yvan-Charvet, L., Even, P., Bloch-Faure, M., Guerre-Millo, M., Moustaid-Moussa, N., Ferre, P., and Quignard-Boulange, A. (2005). Deletion of the angiotensin type 2 receptor (AT2R) reduces adipose cell size and protects from diet-induced obesity and insulin resistance. Diabetes *54*, 991–999.

Yvan-Charvet, L., Massiéra, F., Lamandé, N., Ailhaud, G., Teboul, M., Moustaid-Moussa, N., Gasc, J.M., and Quignard-Boulangé, A. (2009). Deficiency of angiotensin type 2 receptor rescues obesity but not hypertension induced by overexpression of angiotensinogen in adipose tissue. Endocrinology *150*, 1421–1428.